Chapter 5

ATMOSPHERIC TRANSPORT AND DEPOSITION OF MERCURY TO THE ARCTIC REGION

Mercury airborne contamination of the Arctic as a whole and regions of the Russian North are described in this chapter. The assessment is based on the modeling results of mercury long-range transport in the Northern Hemisphere. Since the Arctic is exposed to the adverse impact of distant polluted regions (especially, in the case of such global pollutant as mercury), peculiarities of mercury transport in the Northern Hemisphere are briefly described in the beginning. Particular attention is paid to the effect of Mercury Depletion Events (MDE) on the Arctic pollution based on the accepted parameterization. The consistency of the modeling results is verified by the comparison with available measurements. Further, general features of the Arctic region pollution by mercury are outlined. Finally, detailed description of the Russian North regions pollution by mercury is presented. Concentration levels of mercury in the ambient air and deposition fields are evaluated for all the selected regions. Seasonal variation of the pollution is considered. Main contributors to the contamination of the regions are determined and prevailing pathways of mercury transport are discussed.

5.1. General description of modeling results

Computations of the atmospheric mercury transport and deposition in the Northern Hemisphere have been performed for 1996 by means of the developed model (Chapter 3). The calculation run for the period of one year have been carried out using emission data described in Section 4.1 and the appropriate initial and boundary conditions (Section 3.2). To take into account the long atmospheric residence time of mercury we performed two-year spin-up of the model using the same meteorological data. Results of mercury transport modeling in the Northern Hemisphere are described below.

Concentration levels and deposition fields

Mercury concentration in the ambient air and deposition fluxes to the ground is the primary information characterizing a negative impact of the pollutant on the human health and the environment. Figure 5.1 shows calculated spatial distribution of mean annual concentration of total gaseous mercury (TGM) in the surface air of the Northern Hemisphere. The modelling results presented below are arithmetical means of the calculations obtained using two natural emission and re-emission scenarios (see Section 4.1). Analysis of the difference between two emission scenarios is presented at the end of the section. According to the modeling results TGM is more or less uniformly distributed over the Northern Hemisphere. This fact agrees with numerous measurements carried out for last several decades [e.g. see *Ebinghaus et al.*, 1999]. As seen in the figure TGM concentration in the Northern Hemisphere varies from about 1 ng/m^3 (under local conditions) in elevated remote regions (Greenland, the Himalayas) to some ng/m^3 in industrialized areas. One can clearly distinguish two the most contaminated regions: Eastern Asia with concentrations up to 5 ng/m^3 and Europe (more than 2 ng/m^3). High values of gaseous mercury concentration in these regions can be explained by significant both anthropogenic and natural mercury emissions (see Figs. 5.2 and 5.9). There are pronounced gradients of TGM concentration over the Atlantic and Pacific Oceans. In both cases, concentration decreases from middle latitudes to the equator. It agrees with gradients of TGM measured over the oceans [*Slemr*, 1996; *Lamborg et al*., 2002].

Figure 5.2 demonstrates spatial distribution of particulate mercury (Hg_{part}) in the ambient air. Besides in Southeast Asia and Europe, comparatively high concentrations of particulate mercury occur in Hindustan and the Arabian Peninsula being consistent with the emission data (Fig. 5.2). Due to low amount of precipitation over Africa Hg_{part} flows across this continent and reaches the Atlantic.

Spatial distribution of reactive gaseous mercury (RGM) concentration is shown in Figure 5.3. The residence time of this mercury form in the atmosphere is short due to high solubility and deposition rate. Therefore concentration of gaseous oxidized mercury quickly decreases from regions with major emission sources to remote ones.

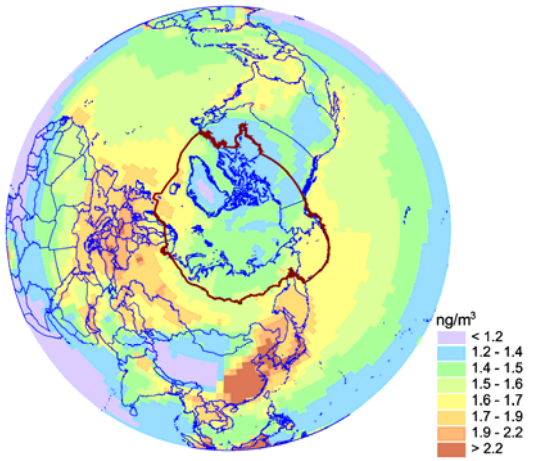

Figure 5.1. *Spatial distribution of mean annual air concentration of total gaseous mercury (TGM) in the surface air of the Northern Hemisphere*

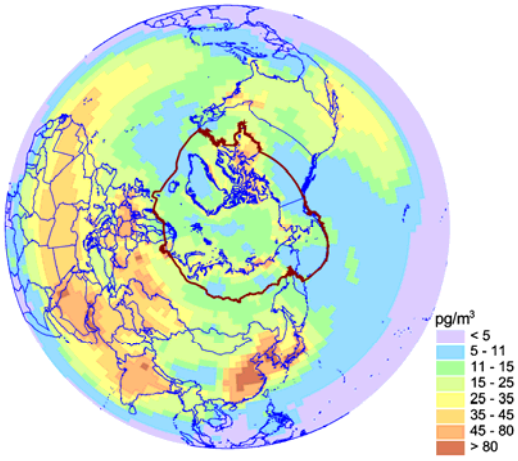

Figure 5.2. *Spatial distribution of mean annual air concentration of particulate mercury (Hg_{part}) in the surface air of the Northern Hemisphere*

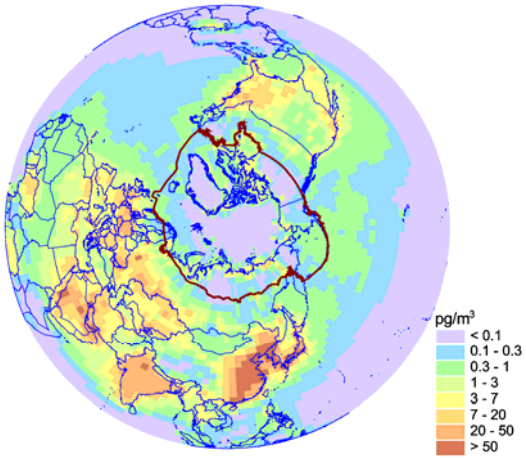

Figure 5.3. *Spatial distribution of mean annual air concentration of reactive gaseous mercury (RGM) in the surface air of the Northern Hemisphere*

Common feature of Hg_{part} and RGM concentration patterns is elevated mercury content in the coastal areas of the Arctic Ocean. This is a direct consequence of the mercury depletion events (MDE). According to the model parameterization of MDE (Section 3.2) during springtime elemental mercury in the lower troposphere is partially transformed to particulate and RGM forms in the vicinity of the Arctic coast. Long-term effect of the phenomenon will be discussed below.

Figure 5.4 presents distribution field of total annual deposition flux of mercury in the Northern Hemisphere. As seen from the figure the most considerable fluxes take place in the middle latitudes. The highest depositions are in the main emission regions: Southeast Asia, Europe, and the eastern part of North America. As for the rest, the deposition pattern, to some extent, corresponds to the annual precipitation amount field, since wet deposition plays a dominating role in the mercury removal process. Influence of MDE on the deposition fluxes within the Arctic region is illustrated in the enlarged fragment. More detailed consideration of the MDE effect is presented in the next subsection.

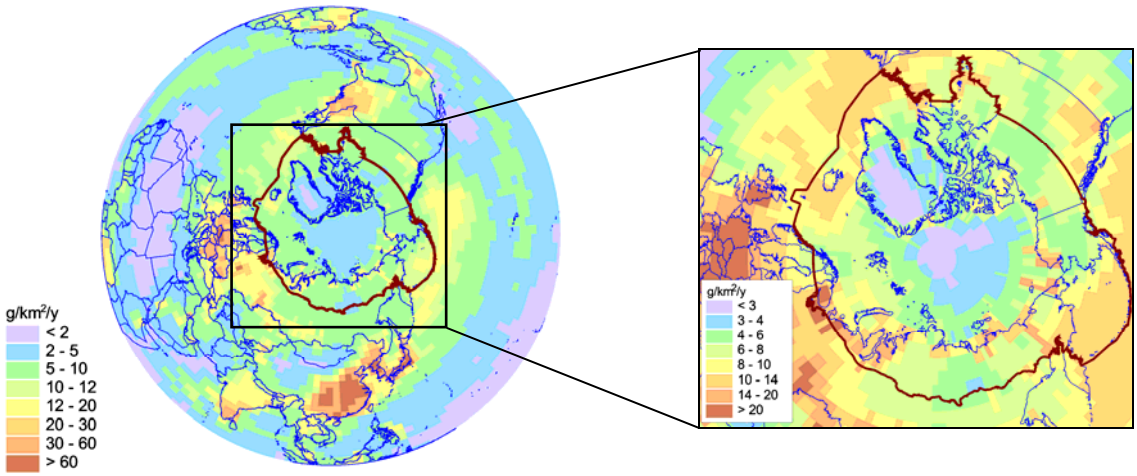

Figure 5.4. *Annual deposition density of total mercury in the Northern Hemisphere. The enlarged fragment shows elevated mercury deposition over the Arctic coast due to MDE*

As it was mentioned in Section 4.1 we performed calculation using two natural emission and re-emission scenarios: Scenario I is the upper limit of the emission estimates; Scenario II is the lower one. It was obtained that differences of mean annual TGM concentration obtained using both scenarios are more noticeable over the ocean because difference between two scenarios of emission from the ocean is more significant (1200 t/y and 500t/y) than that from land (1500t/y and 1100 t/y). Differences of the total deposition flux are insignificant over industrial regions because of considerable contribution of anthropogenically emitted short-lived mercury forms to deposition in these regions. One should note that uncertainty of both TGM concentration and total deposition flux due to uncertainty natural emission and re-emission does not exceed 20% in middle and high latitudes.

Mercury Depletion Events (MDE)

Nature of mercury depletion events taking place during the Arctic sunrise is still unclear to some extent. Proposed hypothesis of the MDE mechanism [*Lindberg et al.*, 2002] includes complicated chemistry involving formation of halogen related radicals. Development of detailed model scheme of MDE phenomenon is the subject of a separate study. In the current research we attempt to estimate roughly long-term effect of MDE on the Arctic pollution using a simplified parameterization (see Section 3.2).

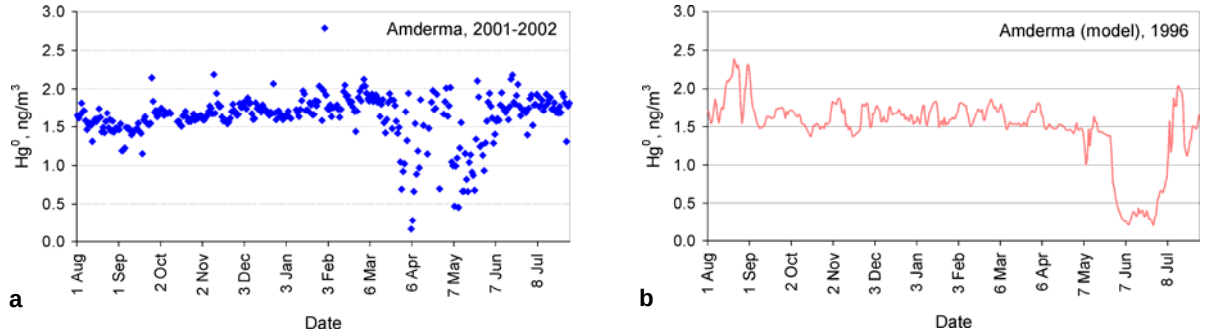

Figure 5.5. *Daily mean air concentrations of elemental mercury at monitoring station Amderma (Russia): (a) – measured in 2001-2002; (b) – modeled on the base of 1996*

The model ability to simulate MDE is illustrated in Figure 5.5. Daily mean concentrations of elemental mercury in air measured in 2001-2002 at monitoring station Amderma (Nenets AO; 69°43'N, 61°37'E)

are presented in Figure 5.5. The measurements were performed within the Joint Canada/Russia project on installation and operation of air monitoring station at Amderma in frame of AMAP (AMAP, Environment of Canada, Air Zone Inc.), and the data was kindly provided by Dr. Konoplev from Center for Environmental Chemistry of SPA "Typhoon" (Russia). As seen from the figure significant drops in elemental mercury concentration takes place at this location in the period from end of March till middle of June. Figure 5.5(b) shows modeled air concentrations of Hg^0 at the same location. Since model calculations were performed for 1996, only qualitative comparison is possible. As one can see from the figure the model reproduces in general the depth of Hg^0 concentration decrease and the duration of the phenomenon. However, simulated MDE phenomenon is shifted in time to summer months due to conditional parameterization of MDE triggering mechanism in the model based on air temperature (Section 3.2). Besides, due to coarse spatial resolution of the model grid it is not able to simulate high variability of Hg^0 concentration during MDE. Nevertheless, the applied approach allows estimating qualitatively long-term effect of MDE on the Arctic pollution taking into account the temporal shift mentioned above.

As it is shown in the enlarged fragment of Figure 5.4 such a short-term phenomenon as MDE, lasting for several weeks per year, can considerably increase annual deposition of mercury in some regions of the Arctic. First of all it relates to marine and terrain areas adjacent to the Arctic coast. To examine the effect of MDE on the Arctic contamination, two computation runs have been conducted. In the first case MDE phenomenon was included into the model, in the second one it was not. The net Influence of MDE on total annual mercury deposition is illustrated in Figure 5.5. The figure shows the difference between deposition fluxes obtained in two computation runs – with and without MDE. As seen MDE can contribute more than 50% to annual deposition to areas adjacent to the Arctic coast (about 300 km northward and southward the coast): the Queen Elizabeth Islands, Hudson Bay, the White Sea, Gulf of the Ob River, the Laptev Sea coast etc. Low negative values show that increased deposition fluxes due to MDE in some regions lead to decreased fluxes in other ones. Thus, a considerable amount of mercury does not reach the pole during springtime being scavenged due to MDE over the coastal and contiguous regions.

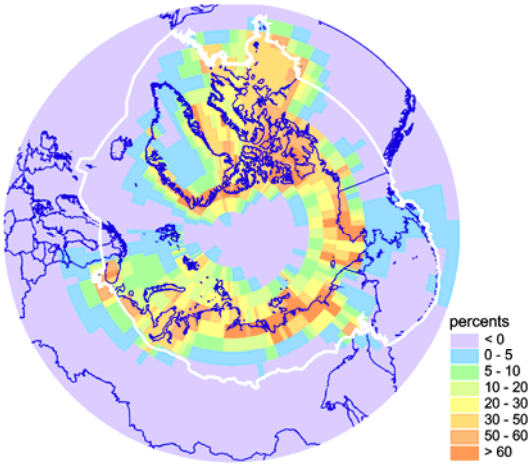

Figure 5.6. *Net Influence of MDE on the total annual mercury deposition. The field presents the difference between two computation runs – with and without MDE. White curve shows limits of the AMAP domain*

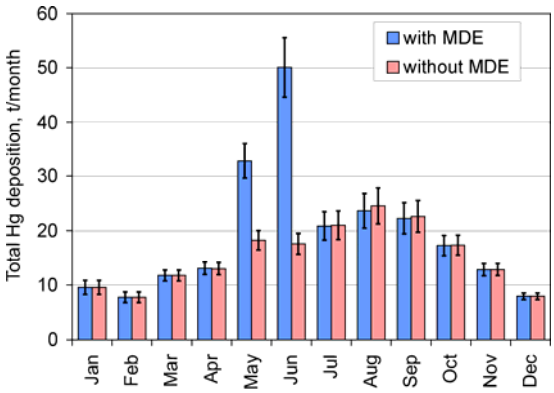

Figure 5.7. *Seasonal variation of total annual mercury deposition to the Arctic with and without MDE. Intervals show difference between two emission scenarios*

Figure 5.7 shows seasonal variation of total annual mercury deposition to the Arctic in both cases. As one can see from the figure, the model predicts the most pronounced effect of MDE in May and June (taking into account the temporal shift mentioned above), when monthly depositions to the Arctic

increased twice or even more. The performed calculations predict that deposition of mercury to the Arctic due to MDE can amount to about 50 t/y (~20% of total annual deposition). It is somewhat lower recent estimates (about 100 t/y) obtained by other authors [*Chistensen*, 2001].

5.2. Comparison of modeling results with measurements

To verify the modeling results the calculated mercury concentrations in the air and deposition fluxes were compared with available monitoring data. Currently, only limited number of measurement data on the annual basis is available for 1996 from the AMAP programme [*Berg and Hjellbrekke*, 1999], the EMEP monitoring network [*Berg and Hjellbrekke*, 1998] and North American NADP/MDN network [*NADP/MDN,* 2002]. The monitoring stations performed regular measurements of mercury in 1996 are listed in Table 5.1. Besides, taking into account restricted number of annual air concentration measurements we included episodic observations and measurements for other years available from the literature. Description of this data is presented in Table 5.2. All sites involved the comparison shown in Figure 5.8.

Table 5.1. *Monitoring stations involved in the model verification*

Station	Code	Latitude	Longitude
AMAP			
Alert	CA420	82°28'N	62°30'E
EMEP network			
Westerland	DE1	54°55'N	8°18'E
Zingst	DE9	54°26'N	12°44'E
Pallas	FI96	67°58'N	24°7'E
Mace Head	IE31	53°19'N	9°54'W
Spitsbergen	NO42	78°54'N	11°53'E
Lista	NO99	58°06'N	6°34'E
Rörvik	SE2	57°25'N	11°56'E
Bredkälen	SE5	63°51'N	15°20'E
Vavihill	SE11	56°01'N	13°09'E
Aspvreten	SE12	58°48'N	17°23'E
NADP/MDN network			
Everglades National Park	FL11	25°23'N	80°41'W
Marcell Experimental Forest	MN16	47°32'N	93°28'W
Waccamaw State Park	NC08	34°10'N	78°25'W
Pettigrew State Park	NC42	35°45'N	76°22'W
Longview	TX21	32°23'N	94°43'W
Brule River	WI08	46°45'N	91°30'W
Popple River	WI09	45°48'N	88°24'W
Trout Lake	WI36	46°03'N	89°39'W

Figure 5.8. *Location of the monitoring sites*

Table 5.2 *Episodic measurement campaigns involved in the model verification*

Location	Year	Observ	Model	Reference
Middle Atlantic (Polarstern '96)	1996	1.33-2.12	1.06-1.67	*Temme et al.*, 2003
Motovsky and Kola Bays,	1996	1.6	1.46	*Golubeva et al*., 2003
Northern Sea Rout	1997	1.1	1.4	
Amderma	2001-2002	1.63	1.37	*Konoplev, 2003*
Quebec (Canada)	1998			*Poisant*, 2000
St. Anicet		1.7	1.43	
L'Assomption		1.79	1.4	
Villeroy		1.62	1.38	
Mingan		1.65	1.3	
Guizhou (China)	Multi-year			*Tan et al.*, 2000
Fanjin Mt.		3.4	2.73	
Leigong Mt.		3.1	2.36	
Kang Hwa Island (Korea)	2001	3.26	2.87	*Kim et al.*, 2002

Figure 5.9 shows observed and modeled mean annual mercury concentrations in the ambient air. Only five annual measurements are available for 1996 (blue bars). Other measurements (green bars) were obtained in short term episodic campaigns (e.g. in Motovsky Bay, Barents Sea, Kang Hwa Island) or relate to other years and, therefore, are less reliable in the comparison. Intervals show uncertainty due to natural emission and re-emission (based on two emission scenarios). As one can see the model adequately reproduces annual air concentrations, however, some underestimation is registered at most of episodic sites. As seen from Figure 5.10 the discrepancy observed and modeled values does not exceed 40% with high correlation coefficient (0.94).

The comparison of the observed and modeled annual wet deposition fluxes is presented in Figure 5.11. As seen from the figure the modelled values satisfactorily conform to the measured ones both for European and for North American stations. Variations due to uncertainty of natural emission are even smaller compared to the air concentrations, because most of the stations are located in industrial regions. Regression analysis of wet deposition fluxes is shown in Figure 5.11. As seen the slope of the regression line is close to unity and the discrepancy for all the stations does not exceed a factor of two (dashed lines). The correlation coefficient amounts to 0.54.

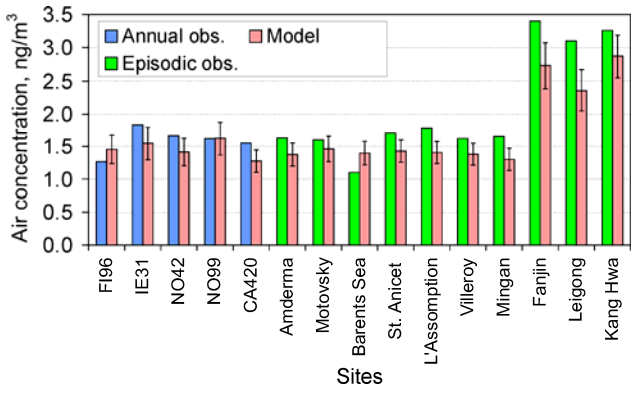

Figure 5.9. *Observed and modeled mean annual TGM concentrations in the ambient air in 1996. Intervals show difference between two emission scenarios*

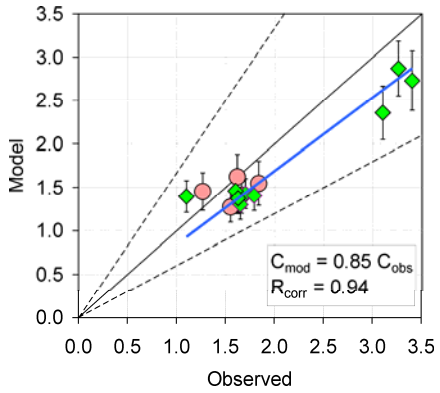

Figure 5.10. *Observed versus modeled mean annual mercury concentrations. Red circles show annual measurements in 1996, green diamonds – episodic campaigns. Dashed lines show discrepancy interval of 40%*

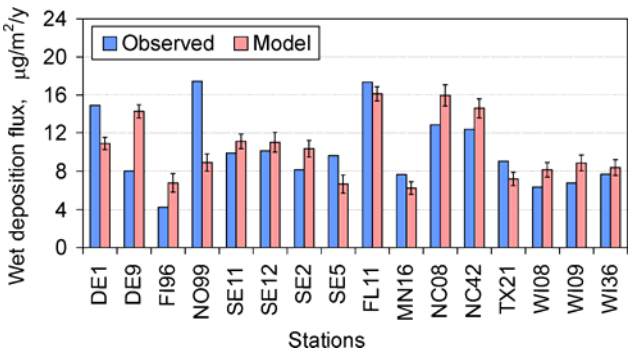

Figure 5.11. *Observed and modeled annual wet deposition fluxes of mercury. Intervals show difference between two emission scenarios*

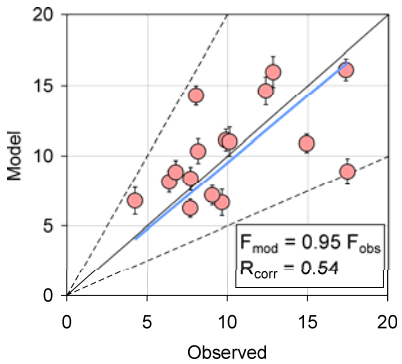

Figure 5.12. *Observed versus modeled annual wet deposition fluxes of mercury. Intervals show difference between two emission scenarios. Dashed lines show discrepancy interval of a factor of two*

To verify the model ability to simulate background mercury concentrations in the ambient air measurement data obtained during the Atlantic cruise on the research ship *Polarstern* in October-November 1996 [*Temme et al*., 2003]. The data was kindly provided by Dr. Franz Slemr from Max-Planck-Institut für Chemie (Germany). The measurements TGM in the surface air were performed during the ship itinerary trough the Northern and Middle Atlantic in the Northern Hemisphere (see Fig. 5.8) and further in the Southern Hemisphere. The original half-an-hour-accumulated data was averaged to obtain daily means. Figure 5.13 shows measured and modeled TGM concentrations over the Atlantic Ocean as a function of geographical latitude. As seen from the figure the model reproduces mercury concentrations close to the observed ones in the Middle Atlantic. More significant discrepancy is in the Northern Atlantic where influence of episodic transport of mercury from anthropogenic sources is possible.

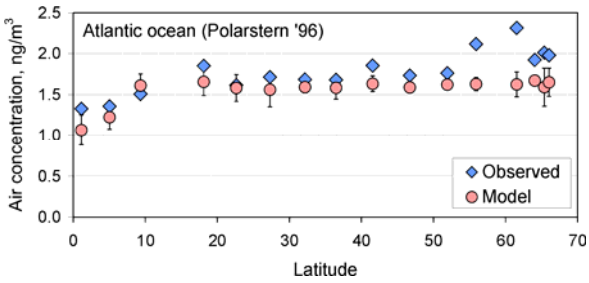

Figure 5.13. *Daily mean concentrations of TGM in the surface layer measured during Polarstern '96 cruise in the Atlantic and modeled for the same locations*

5.3. Arctic region

Mercury contamination of the Arctic has a number of characteristic features peculiar to the region as a whole. In this section we consider general modeled results of the Arctic contamination by mercury.

Levels of concentration and depositions

Figure 5.14 shows levels of mercury concentration in the ambient air of the Arctic region. Here and further we use the AMAP domain limits [*AMAP*, 1998] as a definition of the Arctic region. As seen from the figure air concentration of mercury in the Arctic varies from 1.2 ng/m^3 over Greenland to 2 ng/m^3 in the North Atlantic. Besides, elevated values of concentration occur in the Bering Sea. In the first case this is result of the long-range transport from European sources, in the second one – mainly the influence of mercury sources from Southeast Asia. Mean annual concentrations of mercury over the Arctic Ocean and Asian part of Russia are around 1.5 ng/m^3.

Spatial distribution of annual mercury deposition to the Arctic is presented in Figure 5.15. As one can see, the deposition field varies more significantly – from less than 3 g/km^2 per year in Greenland and near the pole to more than 20 g/km^2 per year over areas adjacent to the Arctic coast. The reasons for that variability are annual precipitation pattern (defining wet depositions) and mercury depletion events. Considerable depositions are also in the North Atlantic and the Bering Sea.

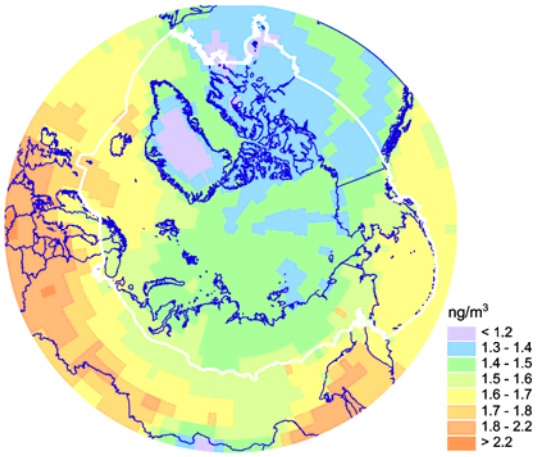

Figure 5.14. *Spatial distribution of mean annual air concentration of total gaseous mercury (TGM) in the Arctic region. White curve shows limits of the AMAP domain*

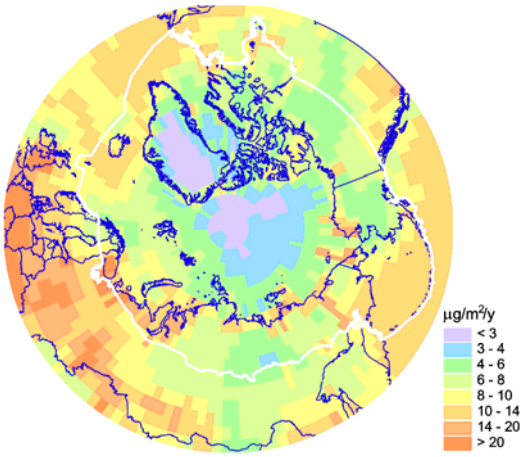

Figure 5.15. *Spatial distribution of total annual deposition of mercury in the Arctic region. White curve shows limits of the AMAP domain*

Main contributors to the Arctic pollution

Due to the high transport potential of mercury in the atmosphere many anthropogenic and natural sources from different regions of the Northern Hemisphere contribute to the Arctic pollution. Figure 5.16 demonstrates relative contributions of anthropogenic and natural sources to the annual mercury deposition to the Arctic. Unidentified sources describe mercury coming through the equator. Here we do not distinguish primary emission sources and re-emission of mercury previously deposited to the ground. As it is seen contribution of anthropogenic sources varies from 40% to 49%, whereas natural sources contributes from 44% to 54%.

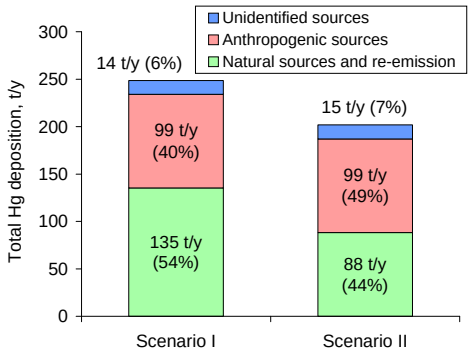

Figure 5.16. *Contribution of different types of sources of the Northern Hemisphere to the annual deposition of mercury to the Arctic. Unidentified sources describe mercury coming through the equator*

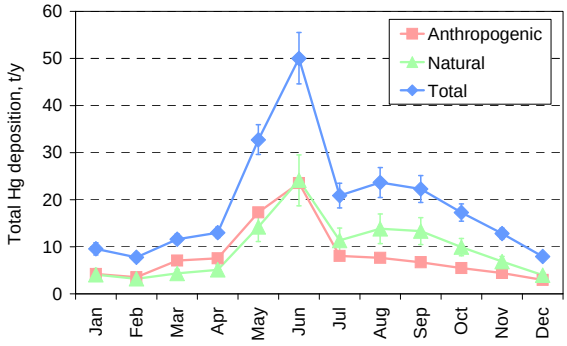

Figure 5.17. *Seasonal variation of total mercury deposition of to the Arctic. Intervals show difference between two emission scenarios*

Seasonal variation of total mercury deposition of to the Arctic is illustrated in Figure 5.17. A significant influence of MDE on the Arctic deposition is predicted in the end of spring and beginning of summer (here one should take account of the temporal shift mentioned in Section 5.1), when total deposition amounts to 50 tonnes per month. Deposition of anthropogenic mercury is defined mostly by variation of precipitation, whereas deposition from natural sources and re-emission is considerably influenced by the temperature dependence of the emission process, it leads to the increase of natural emissions in the late summer.

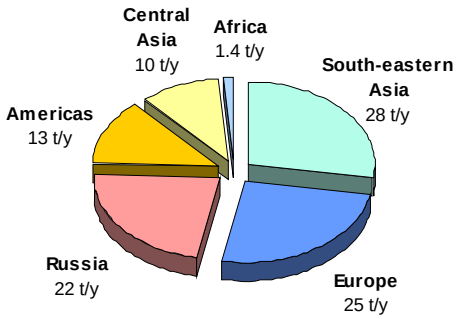

Figure 5.18. *Contribution of different regions to the annual deposition of mercury to the Arctic from* ***anthropogenic*** *sources*

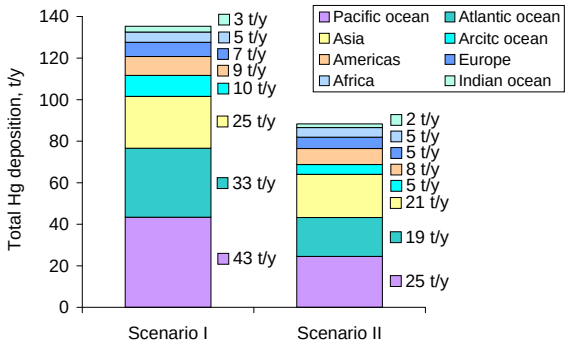

Figure 5.19. *Contribution of different regions to the annual deposition of mercury to the Arctic from* ***natural*** *sources and* ***re-emission***

The contribution of different regions of the Northern Hemisphere to the total annual deposition to the Arctic from anthropogenic and natural sources are shown in Figures 5.18 and 5.19 respectively. As one can see the most significant contributors to anthropogenic mercury deposition are sources located in South-east Asia, Europe and Russia. The most significant contributions to the natural component of annual deposition to the Arctic are from the Pacific and Atlantic oceans, and from Asia. Keeping in mind that the parameterization of natural emission and re-emission processes contain considerable uncertainty and, on the other hand, natural emission cannot be controlled by any political decisions we shall pay more attention to deposition from anthropogenic sources.

5.4. Regions of the Russian North

Mercury contamination of the Russian North contains both common features peculiar to the Arctic region and some distinctions determined by local conditions. This section contains a detailed consideration of contamination of the Russian North regions by mercury. We shall consider five selected regions: Murmansk Oblast (MUR), Nenets AO (NEN), Yamalo-Nenets AO and Taimyr AO (YNT), Sakha Republic (Yakutia) (YAK), and Chukotka AO (CHU).

Levels of concentration and depositions

Figure 5.20 shows spatial distribution of mean annual concentration of TGM in the ambient air of regions of the Russian North. It is seen that mean annual concentration varies slightly over this territory (from 1.4 to 1.8 ng/m^3). There are elevated concentration levels in Murmansk Oblast and in central Sakha Republic related mostly to local emission sources. Besides, there is some gradient of mercury concentration southward in such regions as Yamalo-Nenets AO, Sakha Republic and Chukotka AO. Possible reason is a considerable decrease of elemental mercury concentration over the Arctic coast during springtime caused by mercury depletion events.

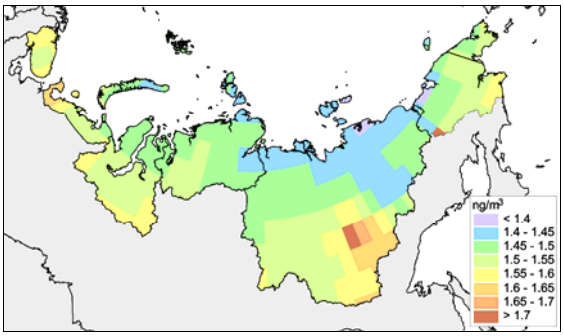

Figure 5.20. *Spatial distribution of mean annual air concentration of TGM in the Russian North*

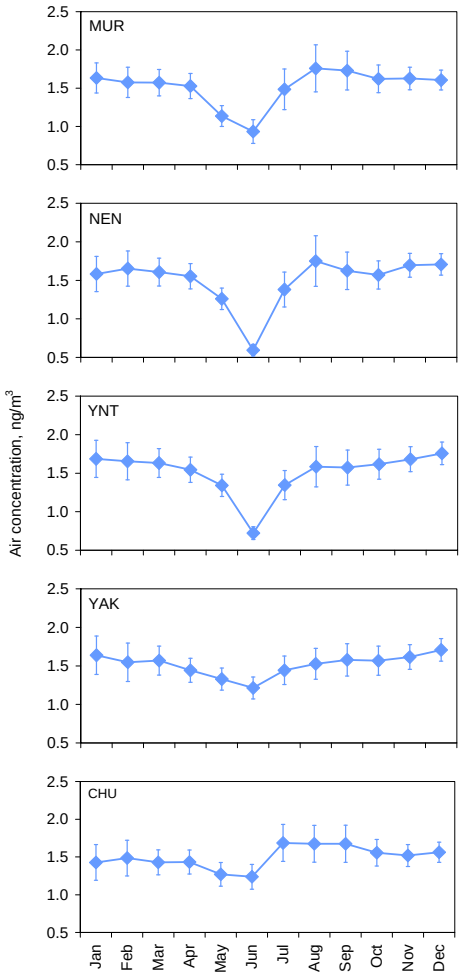

Figure 5.21. *Seasonal variation of average concentration of TGM in the regions of Russian North. Intervals show difference between two emission scenarios*

The effect of MDE on seasonal variation of mercury concentration in the ambient air is illustrated in Figure 5.21. As seen from the figure the lowest concentrations in all the regions are observed in June. The strongest decrease occurs in Nenets AO (down to 0.7 ng/m^3), whereas in Sakha Republic and Chukotka AO it is not so significant (concentration is about 1.4 ng/m^3). The can be explained by large interior territory for the former and significant influence of transport from Asian sources for the latter. Slightly elevated concentrations in last months of summer can be explained by increased natural emission (and re-emission) of mercury in the late summer due to higher surface temperature during this season.

Spatial distribution of mercury air concentration in two different months (June ad December) is illustrated in Figures 5.22 and 5.23. In June (Fig. 5.22) low concentrations (lower than 0.6 ng/m^3) are clearly seen over the Arctic coast due to MDE. The most significant decrease is over Gulf of the Ob River, the Laptev Sea and the East Siberian Sea coasts. High concentration values in the southern part of Sakha Republic and the Pacific coast of Chukotka AO are caused by long-range transport from South-eastern Asia (mostly from China). Concentration levels of mercury in December (Fig. 5.23) are comparatively higher for two reasons: coastal zones are not exposed to MDE phenomenon any more, and lower air temperature leads to higher air density and in turn volume concentrations. Besides, some of the regions (Nenets AO, Yamalo-Nenets AO and Taimyr AO and Sakha Republic) are subjected to a significant influence of Russian and other European sources.

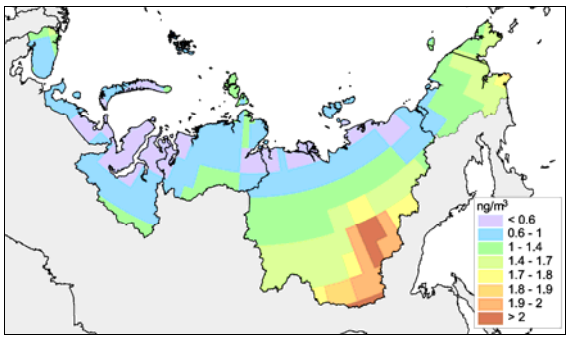

Figure 5.22. *Spatial distribution of monthly mean concentration of TGM in the Russian North in June*

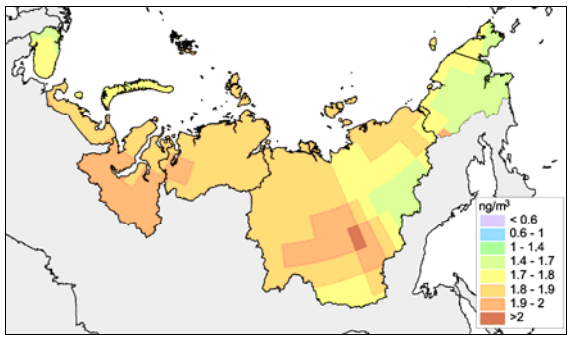

Figure 5.23. *Spatial distribution of monthly mean concentration of TGM in the Russian North in December*

Spatial distribution of total annual deposition flux of mercury is shown in Figure 5.24. The highest depositions are to the coast of the Arctic Ocean due to MDE, where annual deposition flux can exceed 20 g/km^2. The lowest depositions (less then 5 g/km^2/y) are in central Sakha Republic because of a small amount of annual precipitation in this region. Total annual deposition of mercury to Murmansk Oblast is 3 t/y, to Nenets AO - 3.7 t/y, to Yamalo-Nenets AO and Taimyr AO – 14.5 t/y, to Sakha Republic – 20.7 t/y, and to Chukotka AO – 7 t/y.

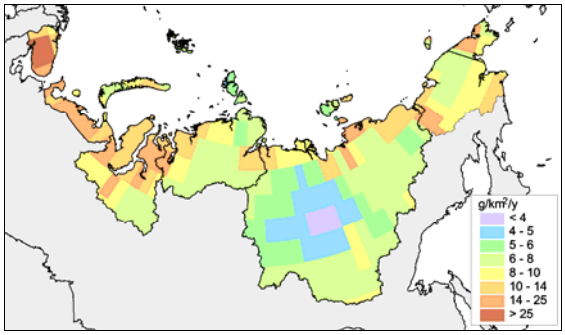

Figure 5.24. *Spatial distribution of annual deposition flux of total mercury to the Russian North*

Seasonal variation of total mercury deposition flux averaged over the regions is illustrated in Figure 5.25. For comparison variation of precipitation amount is also presented. As seen from the figure seasonal variation of deposition in general well correspond to that of precipitation, because wet deposition with precipitation is the dominating mechanism of mercury scavenging from the atmosphere. The exception is high depositions to all regions during May and June when mercury depletion events (MDE) take place. Deposition fluxes in these months can several times exceed those during the rest of the year. The highest exceeding is in Murmansk Oblast, because according to the model parameterization almost all its territory is exposed to MDE (see Fig. 5.6).

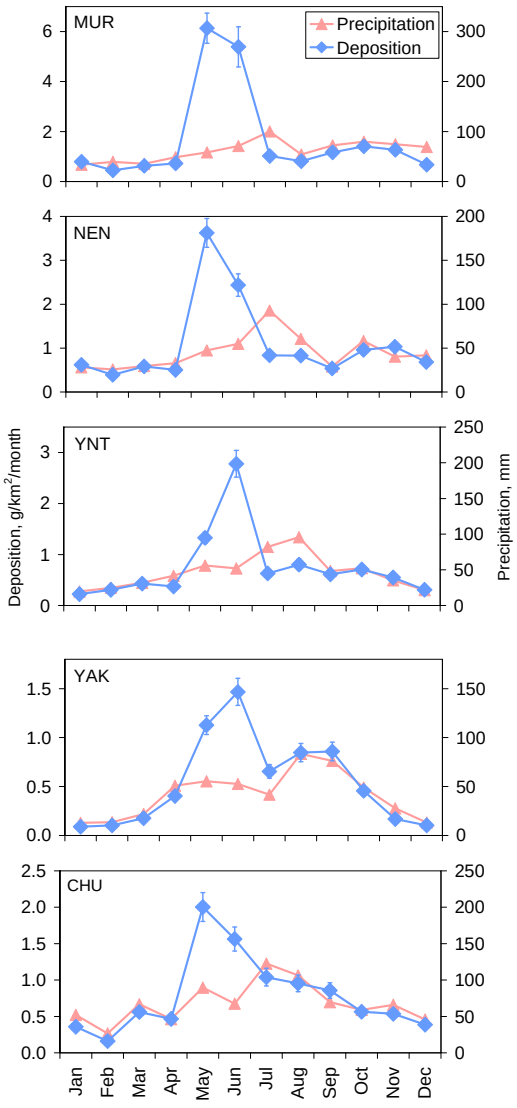

Figure 5.25. *Seasonal variation of average deposition flux of total mercury in the regions of the Russian North. Intervals show difference between two emission scenarios*

Variation of spatial distribution of mercury deposition fluxes during a year is shown in Figures 5.26 and 5.27. As it is expected the most intensive depositions in June (Fig. 5.26) are over areas of the Arctic coast where MDE takes place. In December (Fig. 5.27) depositions are considerably lower in all the regions and especially in Sakha Republic due to low precipitation amount.

Characteristic values of mean annual air concentrations and total annual deposition flux for each region are summarized in Table 5.3.

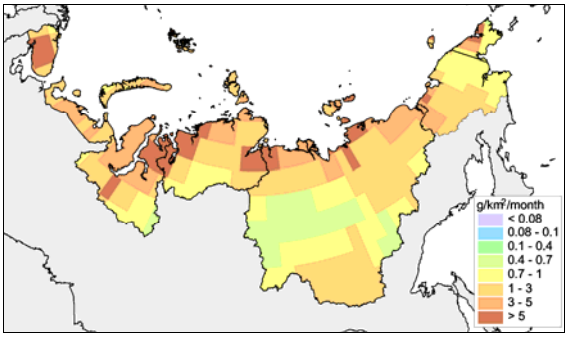

Figure 5.26. *Spatial distribution of monthly deposition flux of total mercury in the Russian North in June*

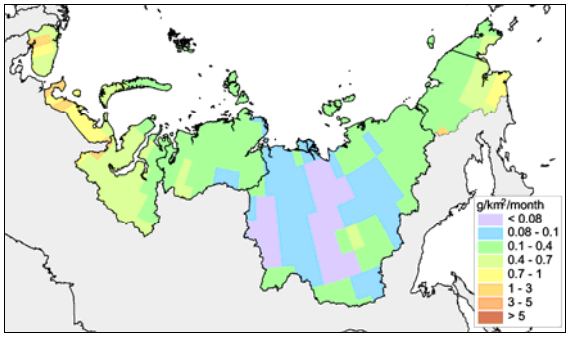

Figure 5.27. *Spatial distribution of monthly deposition flux of total mercury in the Russian North in December*

Table 5.3. *Characteristic values of air concentrations and total annual deposition flux in five selected regions of the Russian North*

Region	Air concentrations, ng/m^3			Total annual deposition flux, g/km^2/y		
	min	max	average	min	max	average
Murmansk Oblast	1.52	1.62	1.56	8	30	21
Nenets AO	1.44	1.66	1.52	6	26	14
Yamalo-Nenets AO and Taimyr AO	1.43	1.58	1.5	5	15	10
Sakha Republic	1.38	1.75	1.5	3	17	7
Chukotka AO	1.38	1.71	1.5	6	18	10

Relative contribution of different regions to the pollution of the Russian North is analyzed in the next subsection. Since methylmercury naturally formed from inorganic mercury by biological activity in aquatic compartments, makes the most significant adverse impact of mercury on the human health and the environment, we shall pay further more attention to deposition of airborne mercury to the surface.

Contribution of different regions to the pollution of the Russian North

Dispersion of mercury in the global atmosphere and, in particular, source-receptor relationships have some peculiarities. Due to long residence time of mercury in the atmosphere (about 1 year) it is able to flow with air mass around the globe (one or more times) until it is deposited to the ground. Therefore pollution of remote regions by mercury, in contrast to short-lived pollutants (e.g. lead), looks not as direct transport from source region to a receptor region but rather as the contribution of locally emitted mercury to the global mercury pool in the atmosphere (so-called 'global background'), mixing, and further deposition to the surface. However, in some cases episodic or seasonal influence of large regional sources on pollution of a certain region can even dominate over the global background.

To determine contributors to the pollution of a certain region of the Russian North we distinguish emission sources located in different regions of the Northern Hemisphere as it was described in Chapter 4. We differentiate sources from Russia, Eastern, Western, Northern and Southern Europe, Central Asia, China, Japan, South-east Asia (without China and Japan), both Americas, and Africa. Besides, Russian sources are subdivided into several regions listed in Table 5.3 along with their codes used in the text. The location of the regions is shown in Figure 5.28.

Table 5.4. *Regions of Russia considered in the source-receptor analysis*

Region	Code
Murmansk Oblast	MUR
Nenets AO	NEN
Yamalo-Nenets AO and Taimyr AO	YNT
Sakha Republic (Yakutia)	YAK
Chukotka AO	CHU
Northern Region	NRT
North-Western region and Kaliningrad Oblast	NWK
Central and Volga-Viatsky regions	CVV
Central-Chernozem, Volga, and North-Caucasian regions	CVN
Ural region	URL
West-Siberian region	WSB
East-Siberian and Far-Eastern regions	ESB

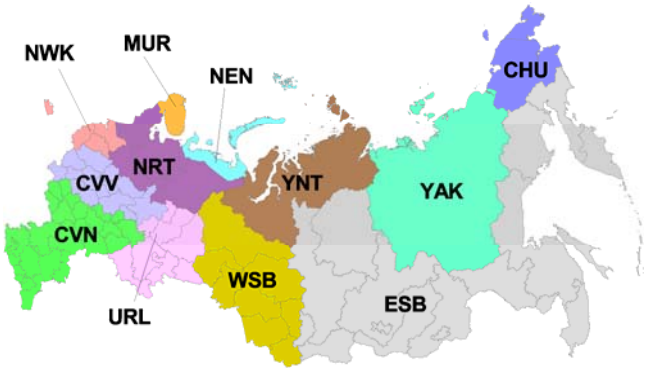

Figure 5.28. *Location of Russian regions*

For the evaluation of source-receptor relationships mercury emitted from each source region is considered separately. However, due to significant number of the source regions (30 including natural sources) calculations for all regions are performed simultaneously. To avoid uncertainties connected with the model non-linearity all the processes (advection, diffusion, chemistry, deposition etc.) are computed for total pollutant mass re-calculating contribution of each source region after each process. Thus, if at some time step contribution of i^{th} source to mercury mass m in a gridcell is α_i and due to some process the mass m is increased by value δm with fraction of i^{th} source β_i, then contribution of i^{th} source to mercury mass in the gridcell at the next time step will be $\alpha'_i = (\alpha_i m + \beta_i \delta m) / (m + \delta m)$. This procedure is performed for each mercury species separately.

Murmansk Oblast (MUR). Murmansk Oblast is one of northwestern regions of Russia located on the Kola Peninsula. That is why influence of European sources (both Russian and external) is most important for this region. Figures 5.29 and 5.30 illustrate contributions of major external and Russian sources to annual mercury deposition to Murmansk Oblast from anthropogenic sources. As seen the largest contribution is made by Russian internal sources (35%). Among them about 13% is from its own sources (MUR) and 18% from other Russian European regions (NRT, NWK, CVV, CVN and URL). The most important external sources are Eastern Europe (12%), China (11%), Americas (10%), and Western Europe (10%). The category "Others" here and for other receptor-regions contains Northern and Southern Europe, South-east Asia (excluding China and Japan), and Africa due to their insignificant contributions.

Figure 5.31 shows seasonal variation of relative contributions of different regions to mercury deposition to Murmansk Oblast. As one can see from the diagram relative contribution of Russian sources is the most variable: It alters from about 50% in February to about 25% in June. This alteration is mainly determined by variation of relative contribution of own sources of Murmansk Oblast (white line). This fact can be explained by the consideration of absolute deposition values (see Fig. 5.32). The absolute value of total deposition from Murmansk Oblast sources varies slightly during the year. Instead, deposition from other Russian regions changes considerably (the same is for external regions).

The reason for increasing contribution of remote sources in May and June is MDE. Indeed, products of MDE (gaseous oxidized and particulate mercury) are the most effectively scavenged from the atmosphere in comparison with other mercury forms.

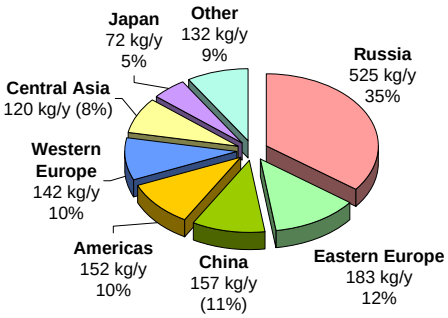

Figure 5.29. *Relative contributions of regions of the Northern Hemisphere to annual mercury deposition to Murmansk Oblast from anthropogenic sources*

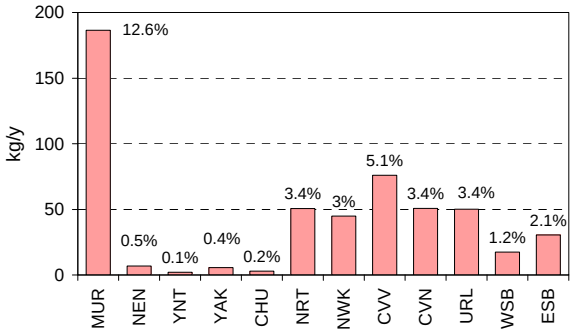

Figure 5.30. *Contribution of Russian regions to annual mercury deposition to Murmansk Oblast from anthropogenic sources*

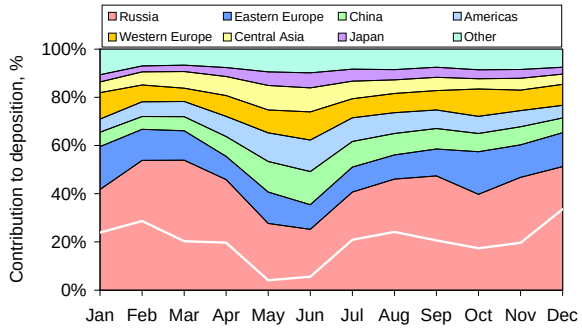

Figure 5.31. *Seasonal variation of relative contributions of different regions to mercury deposition to Murmansk Oblast. White line shows contribution of own sources of Murmansk Oblast*

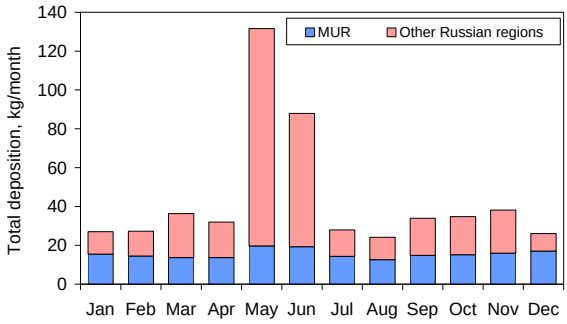

Figure 5.32. *Seasonal variation of total mercury deposition to Murmansk Oblast from anthropogenic sources of Russian regions*

Besides, these forms are also primarily emitted to the atmosphere from anthropogenic sources. Due to a short residence time in the atmosphere gaseous oxidized and particulate mercury are mostly deposited in the vicinity of emission sources. That is why the contribution of MDE to deposition of these forms from local sources is insignificant. On the contrary, mercury from remote sources reaches the region mostly in form of elemental vapour and is not deposited effectively. While during MDE elemental mercury is transformed into short-lived forms and its deposition increases.

In January and October more intensive transport of mercury from European sources takes place (see Fig. 5.31). This transport is illustrated in Figure 5.33 for January.

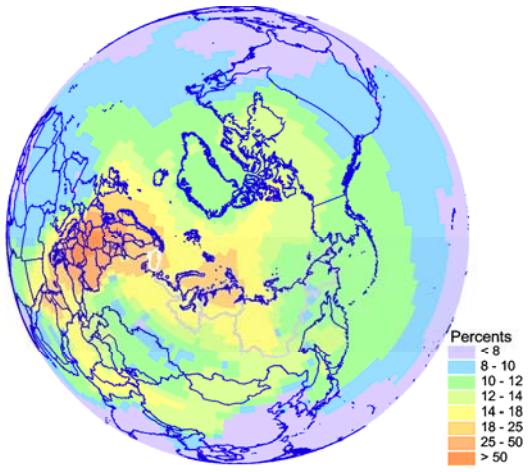

Figure 5.33. *Spatial distribution of relative contribution of East European sources to concentration of anthropogenic mercury in the ambient air in January. White curve shows Murmansk Oblast*

Nenets AO (NEN). Nenets AO is located in the northern part of European Russia. Therefore main features of its long-range pollution are similar to those of Murmansk Oblast. The distinction is more significant influence of Russian regions. Figures 5.34 and 5.35 show the relative contribution of different regions to total annual deposition of mercury to Nenets AO from anthropogenic sources. The largest contribution is made by Russian sources again (35%). However, in comparison to Murmansk Oblast, own sources of Nenets AO contribute only 7% from the total deposition, whereas combined contribution of other Russian European regions (NRT, NWK, CVV, CVN and URL) is more significant (24%). The most important of them are Northern region (NRT), Central and Volga-Viatsky regions (CVV). The most significant external contributors are Eastern Europe (13%), China (11%), Americas (10%), Western Europe (9%), and Central Asia (9%).

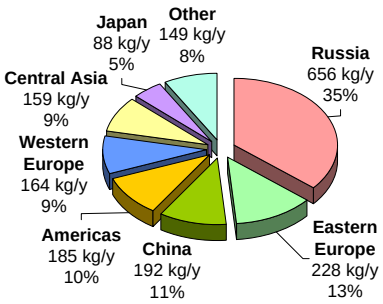

Figure 5.34. *Relative contributions of regions of the Northern Hemisphere to annual mercury deposition to Nenets AO from anthropogenic sources*

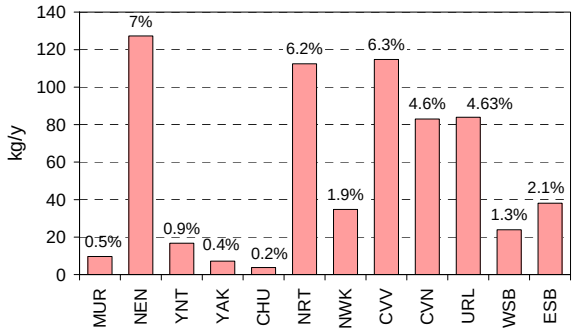

Figure 5.35. *Contribution of Russian regions to annual mercury deposition to Nenets AO from anthropogenic sources*

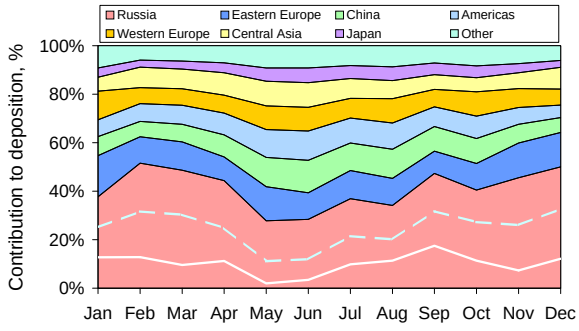

Figure 5.36. *Seasonal variation of relative contributions of different regions to mercury deposition to Nenets AO. White solid line shows the contribution of own Nenets sources, dashed line – combined contribution of three the most important regions (NEN, NRT and CVV)*

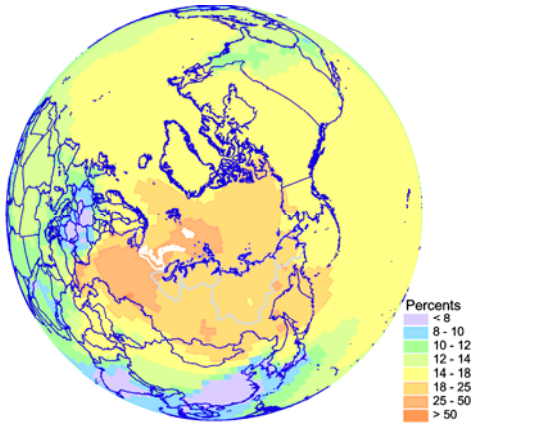

Figure 5.37. *Spatial distribution of relative contribution of Russian European sources (NRT, NWK, CVV, CVN, and URL) concentration of anthropogenic mercury in the ambient air in November. White curve shows Nenets AO*

Seasonal variation of relative contributions from different sources is presented in Figure 5.36. As in the case of Murmansk Oblast the contribution of Russian sources is the most variable. However, in this case the variation is determined not only by own Nenets sources but also by sources from Northern, Central and Volga-Viatsky regions (see dashed line in Fig. 5.36). Beside MDE months (May and June) depositions from these sources are significant in March and November. The transport of mercury from Russian European regions sources (NRT, NWK, CVV, CVN, and URL) in November is illustrated in Figure 5.37. The contribution of all external sources increases during MDE in May and June. Moreover, the transport from Eastern and Western European sources make up some essential contribution in January.

Yamalo-Nenets AO and Taimyr AO. Location of Yamalo-Nenets AO and Taimyr AO in northern part of western Siberia accounts for the fact that Asian sources become play a noticeable role in their pollution, however, European ones still continue to exert a considerable effect. As seen from Figure 5.38 up to 30% of mercury annually deposited to these regions is from Russian sources. One should note that the contribution of own sources of Yamalo-Nenets AO and Taimyr AO is comparatively low (about 3%), whereas three major Russian contributors (CVV, CVN, and URL) make up 16% of total deposition (see Fig. 3.39). Two major external contributors are China (12%) and Eastern Europe (12%). A considerable impact is also from Americas (11%), Central Asia (11%) and Western Europe (9%).

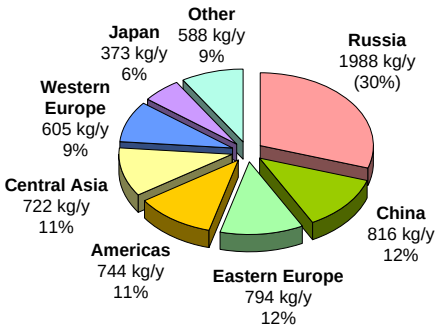

Figure 5.38. *Relative contributions of regions of the Northern Hemisphere to annual mercury deposition to Yamalo-Nenets AO and Taimyr AO from anthropogenic sources*

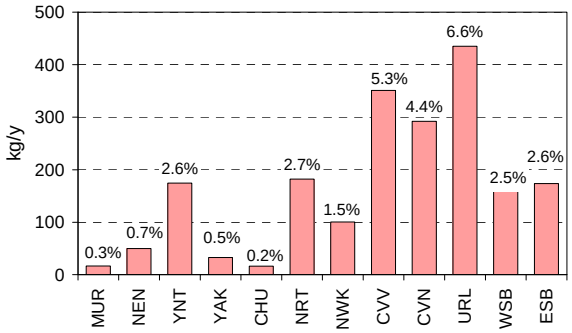

Figure 5.39. *Contribution of Russian regions to annual mercury deposition to Yamalo-Nenets AO and Taimyr AO from anthropogenic sources*

Seasonal variations of relative contributions are shown in Figure 5.40. As seen variation of Russian sources has in general the same shape as those of Murmansk Oblast and Nenets AO (with maximum in February and minima May and June) but with lower amplitude. It could be explained by insufficient influence of own sources (white solid line). On the other hand, the seasonal variation is substantially defined by the impact of one of the main internal contributors – Ural region (dashed line). As usual, contribution of external regions increases during MDE in June. Besides, transport from China affects more significantly in September, Eastern and Western Europe contribute more essentially in January, whereas contribution of Central Asia increases in February and December. Mercury transport from Central Asian sources northward in December is shown in Figure 5.41.

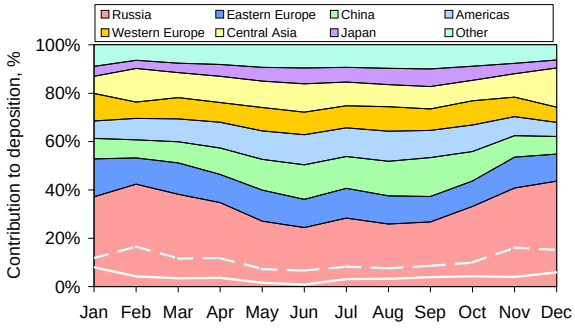

Figure 5.40. *Seasonal variation of relative contributions of different regions to mercury deposition to YNT. White solid line shows the contribution of own sources, dashed line – combined contribution of own and Ural region sources*

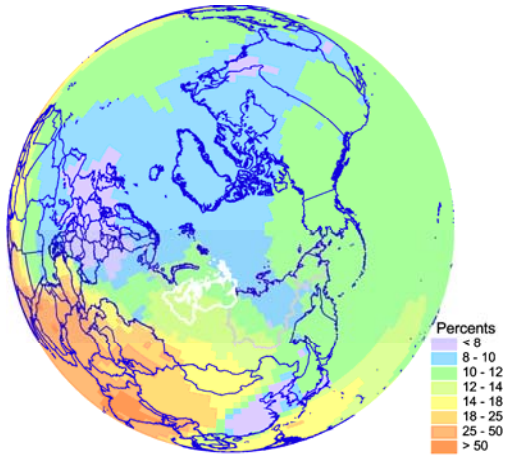

Figure 5.41. *Spatial distribution of relative contribution of Central Asian sources to concentration of anthropogenic mercury in the ambient air in December. White curve shows Yamalo-Nenets AO and Taimyr AO*

Sakha Republic (Yakutia) Sakha Republic is a large region covering the northern and central parts of Eastern Siberia. In spite of insignificant total emission, influence of its own sources is substantial due to a large territory and peculiarities of atmospheric circulation in central Siberia. Besides, Asian sources become dominating in this region. As seen from Figure 5.42 Russian regions contribute about 30% of total annual mercury deposition to Sakha Republic. Among them the most significant contribution is made by own sources of this region (see Fig. 5.43). Major external contributors are China (15%), Americas (11%), Eastern Europe (11%), and Central Asia (10%).

As one can see from Figure 5.44 seasonal variation of the relative contributions are mostly defined by own sources of the region. Their contribution (white solid line) varies from several percent in the beginning of summer up to 20-30% in winter months. Substantial contribution of regional sources in wintertime can be explained by reduced airborne transport to the region due to Siberian Anticyclone traditionally prevailing over winter months. As to external sources, impact of China reaches its maximum in September (up to 20%). Airborne transport of mercury from Chinese sources in September is illustrated in Figure 5.45. It flows northeast from China and reaches Sakha Republic through the Sea of Okhotsk. The contribution of other regions slightly differs from month to month.

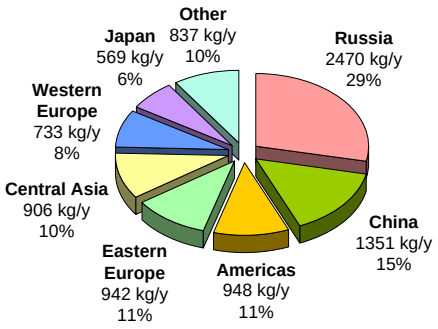

Figure 5.42. *Relative contributions of regions of the Northern Hemisphere to annual mercury deposition to Sakha Republic from anthropogenic sources*

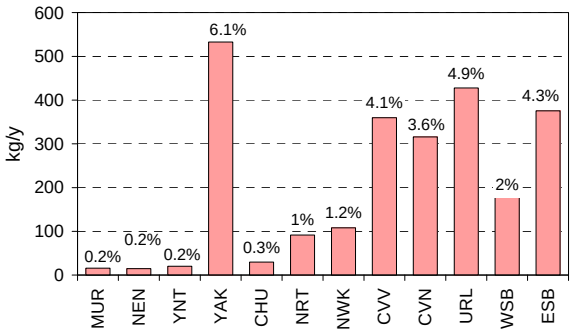

Figure 5.43. *Contribution of Russian regions to annual mercury deposition to Sakha Republic from anthropogenic sources*

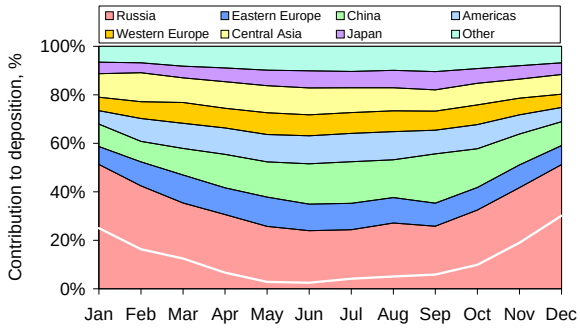

Figure 5.44. *Seasonal variation of relative contributions of different regions to mercury deposition to Sakha Republic. White solid line shows contribution of own sources*

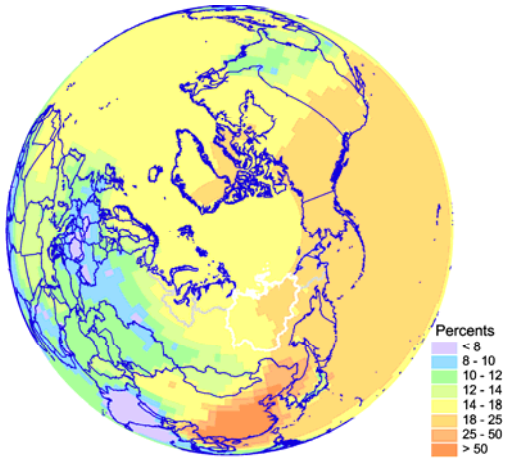

Figure 5.45. *Spatial distribution of relative contribution of Chinese sources to concentration of anthropogenic mercury in the ambient air in September. White curve shows Sakha Republic*

Chukotka AO. Chukotka AO is the most eastward remote region of Russia. Its location far away from major industrial regions accounts for the fact that global background of mercury has a substantial effect on the region pollution. Figure 5.46 demonstrates relative contributions of different regions to annual mercury deposition to Chukotka AO. As seen the main contributor is still Russia (26%), however, contribution of China is also considerable (17%). Among others one can distinguish Americas (11%), Central Asia (10%), and Eastern Europe (10%). The contribution of own sources of Chukotka AO is insignificant comparing with emission sources located in Eastern Siberia and Far East (Fig. 5.47). However, influence of major emission regions from European Russia (CVV, CVN, URL) is also noticeable.

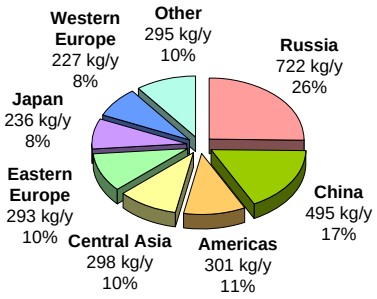

Figure 5.46. *Relative contributions of regions of the Northern Hemisphere to annual mercury deposition to Chukotka AO from anthropogenic sources*

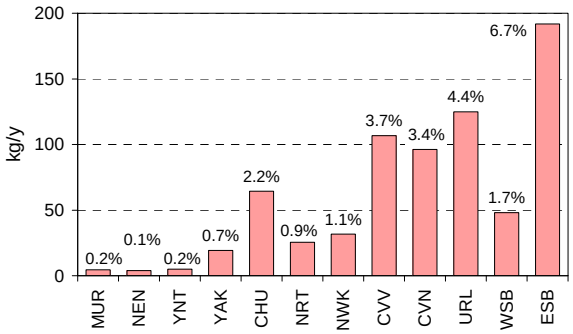

Figure 5.47. *Contribution of Russian regions to annual mercury deposition to Chukotka AO from anthropogenic sources*

As it is shown from Figure 5.48 relative contributions of regions to mercury deposition to Chukotka AO vary slightly during a year. It could be explained by predominance of the global background over episodic transport from neighboring regions. Own sources of Chukotka AO only slightly affect deposition to the region. Russian internal sources permanently make up a substantial contribution (about 20%) with some increase in February due to intensive zonal transport across the entire territory of Russia. Significant mercury depositions to Chukotka AO during of the year are also from Chinese sources. Because of prevailing airflow transport from South-east Asia eastward and north-eastward, Chukotka AO is almost permanently exposed to mercury from Chinese and other Asian sources.

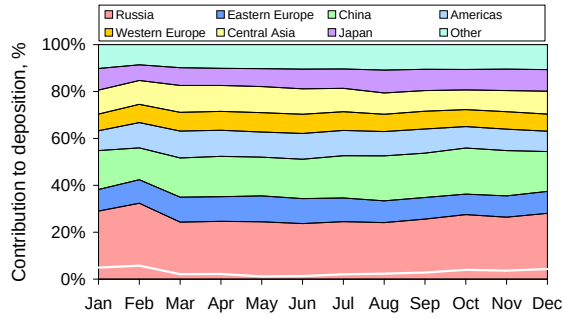

Figure 5.48. *Seasonal variation of relative contributions of different regions to mercury deposition to Chukotka AO. White solid line shows contribution of own sources*

China is one of major emitters of mercury to the atmosphere. Its contribution to the total mercury emission in the Northern Hemisphere makes up to 35% (see Section 4.1). Therefore, influence of Chinese emission sources could be noticeable even for pollution of such remote regions as the Arctic. Figure 5.49 illustrate seasonal patterns of mercury airborne transport to regions of the Russian North from anthropogenic emission sources located in China. As one can see from the figure the dominating direction of the transport from China is eastward to the Pacific. In late winter and spring months its influence is mostly confined by the Pacific Ocean. However, starting from middle of summer mercury from Chinese sources penetrates the Arctic through the Bering Sea and Alaska. In autumn it is transported through the Sea of Okhotsk and attains to eastern regions of the Russian North. In this period contribution of such distinct source region as China to mercury concentration in air of Chukotka AO and Sakha Republic can reach 20%.

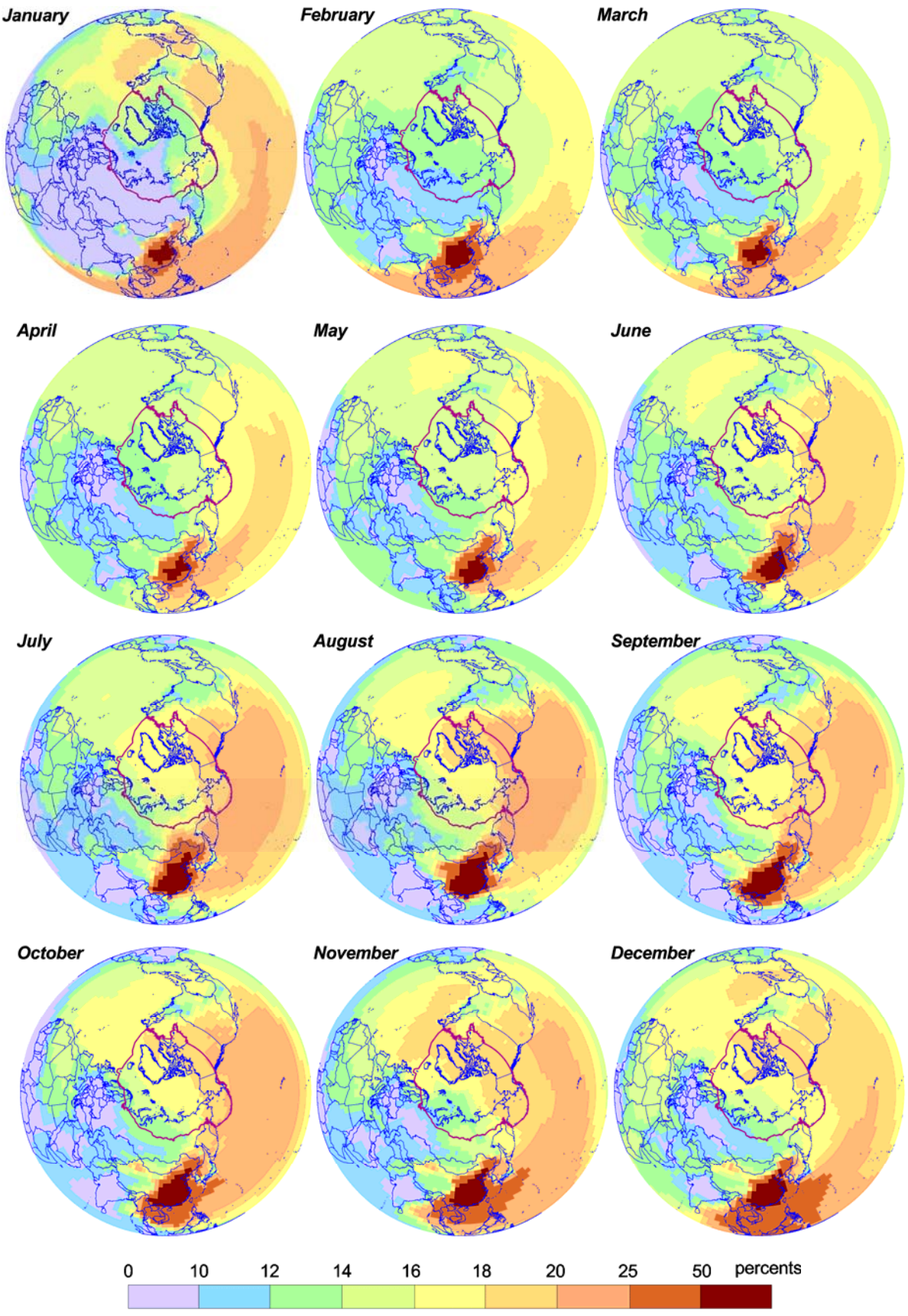

Figure 5.49. *Contribution of Chinese sources to concentration of anthropogenic mercury in the ambient air of the Northern Hemisphere*

5.5. Concluding remarks

Summarizing investigation results presented above one can conclude the following:

- The developed model of mercury long-range airborne transport and depositions on the hemispheric scale can be successively applied to the assessment of mercury concentration levels in the ambient air and deposition fluxes to the surface in the Northern Hemisphere and some particular regions as the Arctic. Satisfactory agreement of modeling results with available measurements verifies reasonable reliability of the model.
- Airborne transport of mercury from remote industrial regions noticeably contributes (up to 40%) to the pollution of the Arctic as a whole and regions of the Russian North, in particular.
- Such short-term phenomenon as mercury depletion events occurring in the Arctic during springtime sunrise does substantially affect the pollution load of this region by mercury considerably increasing (up to 60%) annual mercury depositions in areas adjacent to the Arctic coast (200-300 kilometers northward and southward the coast).
- Natural mercury sources and re-emission of previously deposited mercury are able to contribute considerably to mercury contamination of the Arctic regions. However, the uncertainty of their contributions is still significant.
- Mercury concentration levels in the ambient air slightly vary over all regions of the Russian North (mean annual values 1.4-1.8 ng/m^3). Deposition fluxes vary more significantly (from 4 to 25 g/km^2/y) depending on precipitation amount. The highest depositions are over areas adjacent to the Arctic coast due to mercury depletion events.
- For all regions of the Russian North influence of Russian emission sources dominates over that of external regions. The main external contributors of the Russian North pollution are Eastern and Western Europe, China, Americas, and Central Asia. Relative importance of these contributors varies for different regions of the Russian North. Mercury depletion events phenomenon results in increased role of external sources in the regions pollution.
- Contribution of own regional sources is the most important for **Murmansk Oblast**, but episodic transport of mercury from Eastern and Western European sources can also significantly influence the region pollution.
- Along with own sources of **Nenets AO** emissions from regions of European part of Russia considerably contribute to pollution of this region. Besides, airborne transport from Eastern and Western European sources is also noticeable.
- Ural region and two central regions of European Russia (CVV and CVN) make up the main contribution to the pollution of **Yamalo-Nenets AO and Taimyr AO** from Russian sources, whereas own regional sources do not play a significant role. Main external contributors are China, Eastern Europe, Americas and Central Asia.
- Own regional sources make substantial contribution to pollution of **Sakha Republic**, especially, in wintertime when transport from external sources is reduced. In other seasons episodic transport of mercury from China considerably affect the region pollution.
- Emission sources from Eastern Siberia and Far East are dominating over other Russian regions in regard to mercury contamination of **Chukotka AO**. The main external contributor to the region pollution is China, which contribution is comparable with that of Russian sources and slightly varies during the year.

References

AMAP [1998] *AMAP Assessment report: Arctic pollution issues*. Arctic Monitoring and Assessment Programme (AMAP), Oslo, Norway. 859 p.

Berg T. and Hjellbrekke A.-G. [1998] Heavy metals and POPs within the ECE region. EMEP/CCC Report 7/98, Norwegian Institute for Air Research, Kjeller, Norway

Berg T. and Hjellbrekke A.-G. [1999] AMAP Datareport: Atmospheric subprogramme. NILU OR 16/99, Norwegian Institute for Air Research, Kjeller, Norway

Christensen J. [2001] Modeling of mercury with the Danish Eulerian hemispheric model. International Workshop on Trends and Effects of Heavy Metals in the Arctic. McLean, Virginia, 18-22 June 2001.

Ebinghaus R., Turner R. R., Lacerda de L. D., Vasiliev O., and Salomons W. (Eds.) [1999] *Mercury contaminated sites*. Springer, Berlin. 538 p.

Golubeva N., Burtseva L., Matishov G. [2003] Measurements of mercury in the near-surface layer of the atmosphere of the Russian Arctic. *Sci. Tot. Envir.,* in press

Kim K.-H., Kim M.-Y., Kim J., Lee G. [2002] The concentrations and fluxes of total gaseous mercury in a western coastal area of Korea during late Mart 2001. *Atmos. Environ.* v.36, 3413-3427

Konoplev A. [2003] Private communication.

Lamborg C. H., Fitzgerald W. F., O'Donnell J., and Torgersen T. [2002] A non-steady-state compartmental model of global-scale mercury biogeochemistry with interhemispheric atmospheric gradients. Geochimica et Cosmochimica Acta. v.66, No.7, pp.1105-1118.

Lindberg S. E., Brooks S., Lin C.-J., Scott K. J., Landis M. S., Stevens R. R., Goodsite M., and Richter A. [2002] Dynamic oxidation of gaseous mercury in the Arctic troposphere at polar sunrise. *Environ. Sci. Technol.* v.36, pp.1245-1256

NADP/MDN [2002] *National Atmospheric Deposition Program (NRSP-3)/Mercury Deposition Network*. (http://nadp.sws.uiuc.edu/mdn/)

Poisant L. [2000] Total gaseous mercury in Quebec (Canada) in 1998. *Sci. Tot. Envir.,* v. 259, pp.191-201

Slemr F. [1996] Trends in atmospheric mercury concentrations over the Atlantic ocean and the Wank Summit, and the resulting concentrations on the budget of atmospheric mercury. In: Baeyens W., Ebinghaus R. Vasiliev O. (Eds.), Global and Regional Mercury Cycles: Sources, Flaxes and Mass Balances. NATO-ASI-Series, Kluwer Academic Publishers, Dordrecht, The Netherlands, pp.33-84

Tan H., He J.L., Liang L., Lazoff S., Sommer J., Xiao Z.F., and Lindqvist O. [2000] Atmospheric mercury deposition in Guizhou, China. *Sci. Tot. Envir.,* v. 259, 223-230

Temme C., Slemr F., Ebingaus R., Einax J.W. [2003] Distribution of mercury over the Atlantic Ocean in 1996 and 1999 - 2001, *Atmos. Environ*., in press